Bioconjugate Chemistry

Article

pubs.acs.org/bc

Multifunctional Biocompatible and Biodegradable Folic Acid Conjugated Poly(ε-caprolactone)–Polypeptide Copolymer Vesicles with Excellent Antibacterial Activities

Mingzhi Wang,† Chuncai Zhou,† Jing Chen,† Yufen Xiao, and Jianzhong Du*

School of Materials Science and Engineering, Key Laboratory of Advanced Civil Engineering Materials of Ministry of Education, Tongji University, 4800 Caoan Road, Shanghai 201804, China

Supporting Information

ABSTRACT: Cancer patients after chemotherapy may also suffer bacterial attack due to badly decreased immunity. Although with high bacterial efficacy, conventional antibiotics are prone to inducement of drug resistance and may be not suitable for some cancer patients. In contrast, antibacterial peptides are highly effective in inhibiting bacteria without inducing resistance in pathogens. Presented in this article is a novel kind of highly effective antibacterial peptide-based biocompatible and biodegradable block copolymer vesicle. The copolymer is poly(ε-caprolactone)-*block*-poly[phenylalanine-*stat*-lysine-*stat*-(lysine-folic acid)] [PCL_{19}-*b*-poly[Phe_{12}-*stat*-Lys_9-*stat*-$(Lys\text{-}FA)_6$]], which can self-assemble into vesicles in aqueous solution. The biocompatible and biodegradable PCL forms the vesicle membrane, whereas the poly-[Phe_{12}-*stat*-Lys_9-*stat*-$(Lys\text{-}FA)_6$] block constitutes the vesicle coronas. Compared to the individual polymer chains, the vesicles showed enhanced antibacterial activities against both Gram-positive and Gram-negative bacteria (16 μg mL^{-1}) due to the locally concentrated antibacterial poly[Phe_{12}-*stat*-Lys_9-*stat*-$(Lys\text{-}FA)_6$] coronas, which may avoid the inducement of antibiotic-resistant bacteria and side effects of multidrug interactions. Furthermore, folic acid is introduced into the vesicle coronas for potential further applications such as cancer-targeted drug delivery. Moreover, the amino groups can be further functionalized when necessary. This low cytotoxic, biocompatible, biodegradable, and antibacterial vesicle (without antibiotic resistance) may benefit patients after tumor surgery because it is highly anti-inflammatory, and it is possible to deliver the anticancer drug to tumor cells simultaneously.

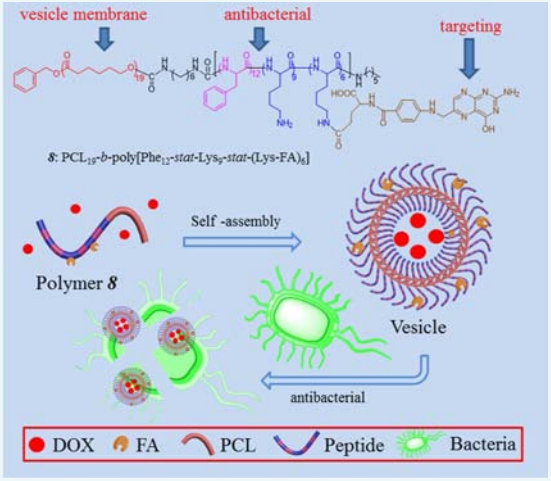

INTRODUCTION

The abuse of conventional antibiotics has led to the emergence of drug resistant pathogens.[1−3] Compared with conventional antibiotics, natural antibacterial peptides showed excellent properties such as limited propensity to induce resistance in pathogens, broad spectrum activity, and rapid onset of killing.[4−6] However, the swinging efficacy, excessive cytotoxicity, and expensive production restricted the antibacterial applications of those peptides.[7] In contrast, *N*-carboxyanhydride (NCA) ring-opening polymerization is an effective and convenient way to synthesize peptides on a large scale.[8] Some peptide-based materials have been synthesized through this method.[9,10] However, only very limited antibacterial peptides have been synthesized by this method.[6,11−13]

Cancer is one of the most dangerous diseases in the world, and chemotherapy is one of the most promising methods for cancer treatment.[14−16] Polymer vesicles have a water pool, a membrane barrier surrounded by hundreds and thousands of hydrophilic coronas.[17,18] Recently, polymer vesicles have been designed for targeted drug delivery and release with high efficiency.[19−23] They have endless applications in morphological phase transition, biomembrane mimics, cosmetics, medicine, etc.[24−27] Compared with solid antibacterial nanoparticles,[28−31] these hollow vesicles are able to carry a range of drugs such as anticancer doxorubicin (DOX) in the bloodstream and release them into cancer cells to avoid direct exposure to the immune system and to decrease cytotoxicity.[32−34]

More importantly, cancer patients are vulnerable to bacterial attack after chemotherapy due to badly decreased immunity.[31] Inflammatory cells can also influence the progress of cancer metastasis.[35,36] Thus, it is necessary to avoid infection during cancer therapy. For example, we recently proposed a new polymer vesicle which can act as an "armed" drug carrier because the vesicle itself has excellent antibacterial activities, which can minimize the possible multiple drug interactions.[13]

In this article, we further anchor an active targeting system on a new antibacterial polymer vesicle (Scheme 1) based on a

Received: January 29, 2015
Revised: February 24, 2015
Published: February 27, 2015

DOI: 10.1021/acs.bioconjchem.5b00061
Bioconjugate Chem. 2015, 26, 725−734

Scheme 1. Illustration of DOX-Loaded Antibacterial Polymer Vesicles with Potential Anticancer Activity[a]

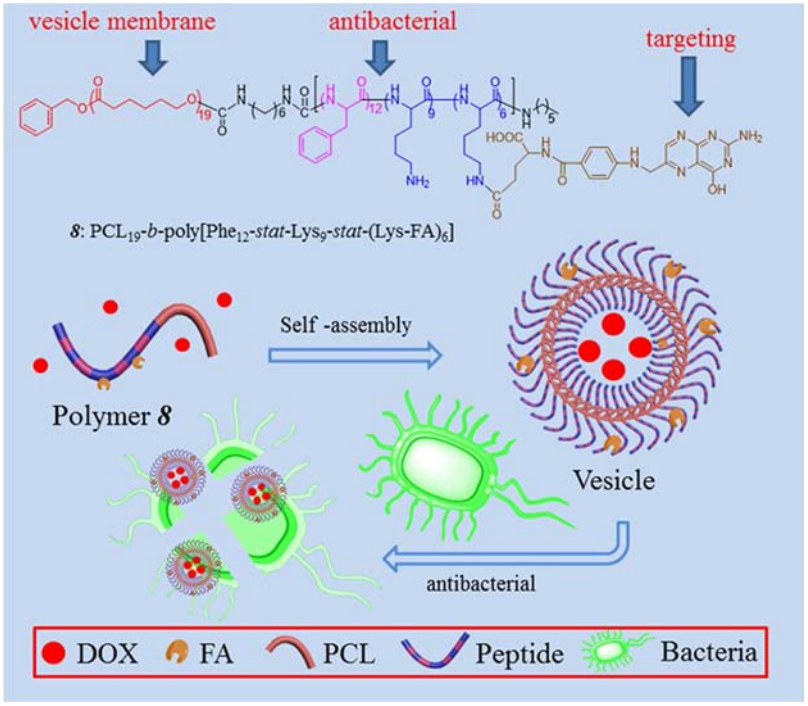

[a]Vesicles composed of hydrophilic coronas (blue and pink) and a hydrophobic membrane (red) are self-assembled from PCL_{19}-*b*-poly[Phe_{12}-*stat*-Lys_9-*stat*-$(Lys\text{-}FA)_6$] (polymer ***8***). The vesicles have excellent antibacterial activities against both Gram-negative and Gram-positive bacteria. The antibacterial vesicles may deliver a range of drugs such as anticancer DOX. The cancer-targeting units (FA) are conjugated by reaction with partial $-NH_2$ groups in the vesicle coronas for potential cancer-targeted drug delivery.

new biodegradable and biocompatible block copolymer, poly(ε-caprolactone)-*block*-poly[phenylalanine-*stat*-lysine-*stat*-(lysine-folic acid)] [PCL_{19}-*b*-poly[Phe_{12}-*stat*-Lys_9-*stat*-$(Lys\text{-}FA)_6$]] (polymer ***8*** in Scheme 2). The FDA-approved biocompatible and biodegradable PCL is designed as the membrane of vesicles. The antibacterial poly[Phe_{12}-*stat*-Lys_9-*stat*-$(Lys\text{-}FA)_6$] forms the vesicle corona with low cytotoxicity. Lysine (Lys) possesses positive charge when placed in water, and then it can adhere to the bacterial membrane, which brings phenylalanine (Phe) an opportunity to penetrate the cell membrane. Once the outer membrane disorganizes, the lysis of cells occurs, resulting in the death of the bacteria.[37,38] This type of antibacterial mechanism will not trigger the increase of drug resistance. Furthermore, the cancer-targeting folic acid (FA)[39−41] on the vesicles may target the cancer cells via FA receptor recognition on the membrane. Moreover, the attractive electrostatic interaction between the vesicle and the cell membrane can facilitate this process. Then, the vesicles can be internalized through endocytosis and release the loaded DOX·HCl to the cell nucleus after the rupture of the endosomal membrane.[42] After degradation, the polymers can be excreted by metabolism in a relatively safe way.

Compared to our previous chitosan and polypeptide-based antibacterial vesicles,[13] besides the excellent antibacterial properties, low cytotoxicity, and good biocompatibility, this new "armed" polymer vesicle has the following advantages: First, the active cancer-targeting unit (FA) has been designed in the vesicle coronas, which provides potential cancer-targeted drug delivery ability. Second, PCL is a cheap biomaterial. Third, the vesicles in this work are very stable in fetal bovine serum (FBS) and phosphate buffered solution (PBS), and have very low critical vesiculation concentration (CVC), providing broader practical applications *in vivo*.

RESULTS AND DISCUSSION

Preparation of Block Copolymers. In this article, a novel antibacterial polypeptide-based polymer with low cytotoxicity and high antibacterial activity has been synthesized in five steps (Scheme 2): (a) Poly[$(Z\text{-}Lys)_{15}$-*stat*-Phe_{12}] (polymer ***3***) was synthesized by NCA copolymerization of Z-Lys-NCA (monomer ***1***) and Phe-NCA (monomer ***2***) using *n*-hexyl amine as the initiator;[8,13] (b) polymer ***3*** with a $-NH_2$ end group reacted with excessive hexamethylene diisocyanate (HDI) at room temperature to form poly[$(Z\text{-}Lys)_{15}$-*stat*-Phe_{12}]-NCO (polymer ***4***); (c) PCL_{19}-OH (polymer ***5***; Figure S5, Supporting Information; M_n 4885; M_w/M_n 1.2) with a −OH end group was synthesized by the ring-opening polymerization (ROP) of ε-caprolactone using benzyl alcohol as the initiator; (d) polymer ***4*** was connected to polymer ***5*** by the reaction of the −NCO group with the −OH group using dibutyltin dilaurate as the catalyst to afford PCL_{19}-*b*-poly[Phe_{12}-*stat*-$(Z\text{-}Lys)_{15}$] (polymer ***6***); and (e) the Z group in polymer ***6*** was deprotected in the HBr/CH_3COOH solution to achieve PCL_{19}-*b*-poly(Phe_{12}-*stat*-Lys_{15}) (polymer ***7***). Then PCL_{19}-*b*-poly[Phe_{12}-*stat*-Lys_9-*stat*-$(Lys\text{-}FA)_6$] (polymer ***8***) was obtained when 40% of Lys in polymer ***7*** was grafted by FA targeting units.

The ^1H NMR spectra of polymers ***3***, ***5***−***7*** in DMSO-d_6 and the corresponding analyses are provided in the Supporting Information (Figures S1−S5). However, it is very difficult to get a good GPC result for polymer ***8*** because this polymer cannot be well dissolved in most of the GPC eluents. Fortunately, the ^1H NMR spectrum confirmed the formation

DOI: 10.1021/acs.bioconjchem.5b00061
Bioconjugate Chem. 2015, 26, 725−734

Scheme 2. Synthesis Strategy toward the Antibacterial Polypeptide-PCL Copolymer

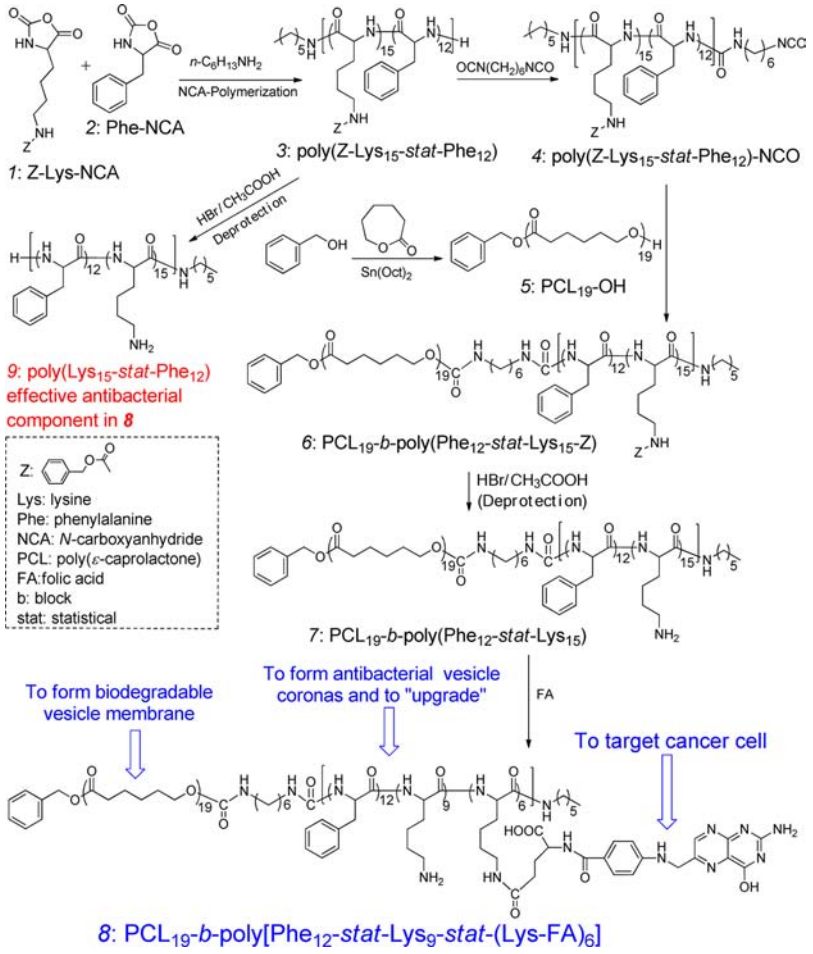

of polymer ***8***, as shown in Figure 1. The characteristic peaks of FA of polymer ***8*** can be detected qualitatively (Figure 1 and Supporting Information, Table S5). Each polymer ***8*** chain was attached with four FA.

Preparation of Block Copolymer Vesicles. Polymer ***8*** can be dissolved in the DMSO with a drop of trifluoroacetic acid (TFA) to break the hydrogen bonding. The copolymer can self-assemble into vesicles in DMSO/water (1:2; v/v). DMSO and TFA can be removed by dialysis against water after self-assembly.

Transmission electron microscopy (TEM) studies confirm the vesicular structure based on the self-assembly of polymer ***8*** (Figure 2). The morphology of the vesicles has been also evaluated by atomic force microscopy (AFM), as shown in Figure S6 in the Supporting Information. The diameter and the height of the vesicles are 323 and 44 nm, respectively. This is because the soft and deformable vesicles collapse on the silicon substrate to show a large diameter/height ratio of 7.34, indicating a hollow structure.[13]

The dynamic light scattering (DLS) study of vesicles from polymer ***8*** is shown in Figure 3. The corresponding mean hydrodynamic diameter (D_h) is 300.8 nm, which is reasonably bigger than that the sizes determined by AFM and TEM.

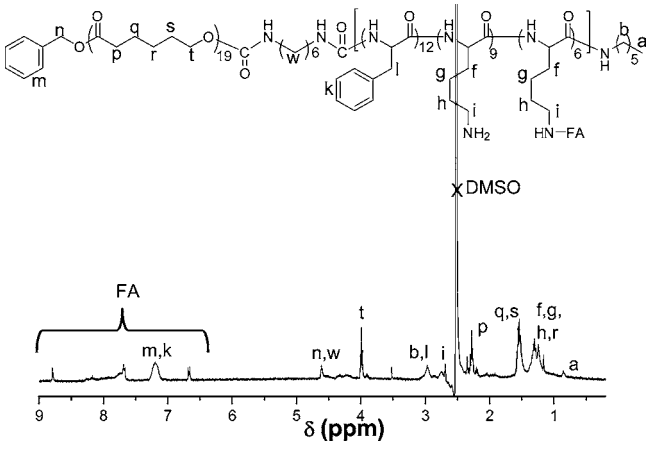

Figure 1. ^{1}H NMR spectrum of PCL_{19}-*b*-poly[Phe_{12}-*stat*-Lys_9-*stat*-$(Lys\text{-}FA)_6$] (polymer ***8***) in d_6-DMSO.

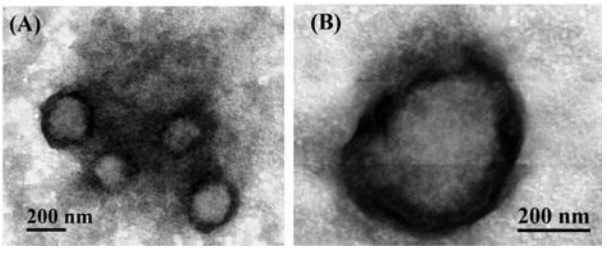

Figure 2. TEM images of polymer ***8*** vesicles stained by 1% phosphotungstic acid (PTA).

DOI: 10.1021/acs.bioconjchem.5b00061
Bioconjugate Chem. 2015, 26, 725−734

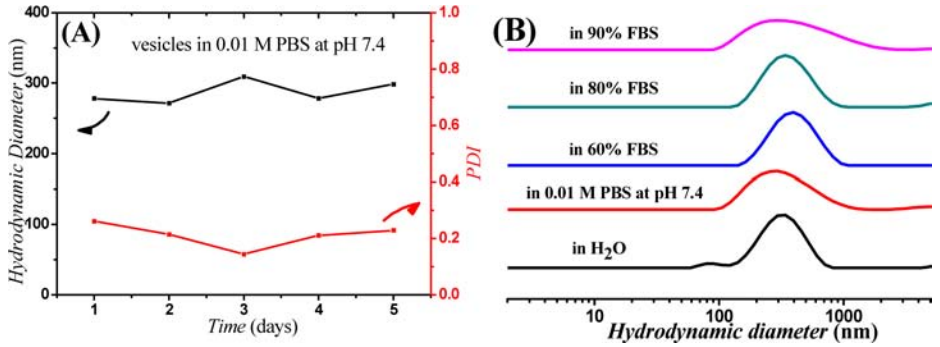

Figure 3. Stability of polymer ***8*** vesicles determined by DLS at 0.5 mg mL^{-1} and 25 °C. (A) Effect of time on the vesicle size in 0.01 M PBS at pH 7.4; (B) Size distribution of vesicles in FBS, PBS, and H_2O. The DLS data are based on intensity.

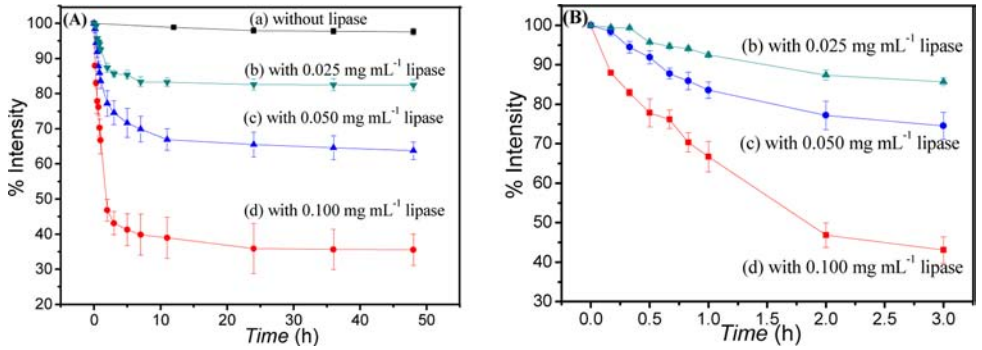

Figure 4. Count rate variation of polymer ***8*** vesicles during enzymatically catalyzed degradation. The function is determined by DLS at 37 °C and pH 7.4. The concentration of vesicles is 0.050 mg mL^{-1}. Panel B is the zoomed-in view of A from 0 to 3 h in the presence of lipase.

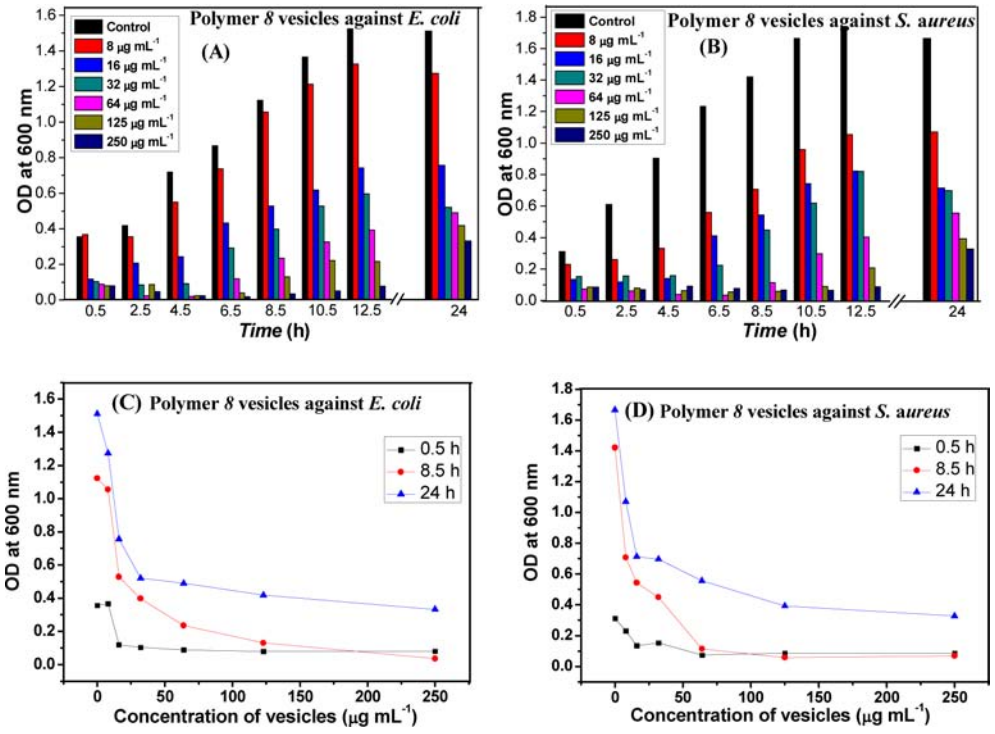

Figure 5. Dose-dependent growth inhibition of a range of bacteria in the presence of vesicles made from polymer ***8***. OD: optical density.

To evaluate their stability under physiological conditions, the polymer ***8*** vesicles were dispersed in phosphate 0.01 M buffered saline (PBS; pH 7.4) and different concentrations of fetal bovine serum (FBS) *in vitro* for 60 h. The vesicle size distribution was monitored by DLS. As shown in Figure 3 and Figure S6 in the Supporting Information, there are no obvious size changes over several days, demonstrating excellent stability in PBS and FBSs.

In Vitro **Enzymatic Biodegradation.** The *Pseudomonas* lipases may result in the degradation of central PCL. PCL is a

DOI: 10.1021/acs.bioconjchem.5b00061
Bioconjugate Chem. 2015, 26, 725−734

good kind of enzymatic degradation material, which is very stable in the normal circumstance through a surface erosion mechanism.[43,44] The PCL has constructed the shell of the vesicles. After the PCL was degraded, the vesicles were disassembled at the same time.

The degradation rates are proportional to the concentration of vesicles, so the process can be evaluated by measuring the decrease in the derived count rate of DLS with time. As shown in Figure 4A, partial PCL chains were hydrolyzed very quickly because the derived count rate decreased very quickly in a short time.

A blank curve indicated the relatively stable vesicular structure in the absence of lipase. Curve a in Figure 4A illustrated the good stability of vesicles without catalysts. In contrast, in the presence of lipase, the vesicles can be quickly degraded (curves b, c, and d in Figure 4A). Furthermore, the degradation rate can be accelerated at higher lipase concentrations (see Figure 4B). However, over a long period of time the polymer vesicles were degraded into peptide and hydroxycarboxylic acid.

Antibacterial Activity. The peptide chains are responsible for the antibacterial activity. The bare amino groups in Lys are positively charged in aqueous solution, while the membranes of bacteria and cancer cells are negatively charged. The electrostatic attraction enables the interaction with bacteria or cell membranes more efficiently.

As a control of the antibacterial polymer vesicles, the antibacterial properties of polypeptides (polymer ***9***) against Gram-negative *E. coli* (ATCC35218) and Gram-positive *S. aureus* (ATCC29213) bacteria were evaluated first. The minimal inhibitory concentration (MIC) is an important index indicating the property of antibacterial activity. The MIC is defined as the minimum inhibitory concentration of an antimicrobial that can inhibit the growth of bacteria. The exact value was obtained by the vesicle solution whose bacteria growth was less than half of the one that contains bacteria only. The lowest concentration of polypeptide inhibiting both *E. coli* and *S. aureus in vitro* after 18 h was 32 μg mL^{-1}.

To evaluate the dynamic antibacterial activity of polymer ***8*** vesicles, MICs were measured using a colony formation assay. The microbial solution was diluted with an appropriate dilution factor in lysogeny broth, then the polymer vesicles solution at various concentrations was added to the lysogeny broth in a cuvette. The solution with bacteria and vesicles was incubated for 24 h at 37 °C, whose optical density was measured at 600 nm of wavelength at intervals. Figure 5A and B revealed the growth rates of bacteria under different conditions. Meanwhile, the plots of bacterial growth rate against polymer concentration at three representative times are provided in Figure 5C and D. The optical density indicates the viability of bacteria, and the black column in Figure 5 is the control with the broth-containing bacteria only. The MICs of polymer ***8*** vesicles against both Gram-negative *E. coli* and Gram-positive *S. aureus* were 16 μg mL^{-1}, which is only half of polymer ***9*** and consistent with our previous studies where we had proven that the assembly of polymers can significantly enhance their antibacterial activities due to the concentration of local cationic charges.[13]

In this study, if we convert the MICs of the whole polymer ***8*** to the effective antibacterial peptide (polymer ***9***) in polymer ***8*** vesicles, the MICs will further decrease to 6.85−9.21 μg mL^{-1}, which are only ca. one-third of that of polymer ***9***. This further confirmed the synergistic effect between PCL (without antibacterial activity) and the antibacterial polypeptide.

The critical vesiculation concentration of polymer ***8*** is 12.88 μg mL^{-1} (see Figure 6). This value is lower than the MIC value (16 μg mL^{-1}), confirming that it is the vesicle not the individual polymer chains that inhibits bacteria in aqueous solution.

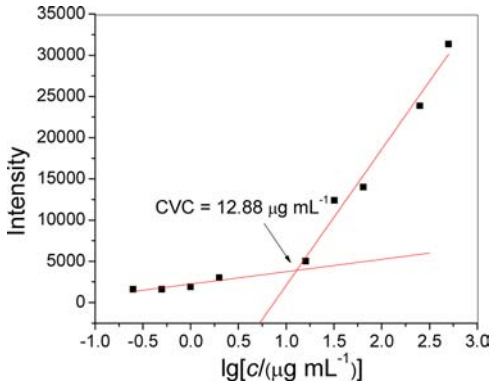

Figure 6. Determination of the critical vesicle formation concentration of polymer ***8***.

Anticancer Drug Loading and Release. DOX loading and release experiments were conducted to evaluate the potential drug delivery behavior of polymer ***8*** vesicles. The interaction between DOX and the hydrophobic membrane of vesicles has facilitated the loading process, which achieved a relatively high drug loading efficiency (DLE). The DLE of vesicles was determined using fluorescence spectroscopy. The drug loading content (DLC) and DLE were calculated according to the following equations.

$$\text{DLC}\ (\%) = \frac{\text{weight of drug encapsulated in vesicles}}{\text{weight of polymer}} \times 100\%$$

$$= \frac{52.9\ \mu\text{g mL}^{-1} \times 23.7\ \text{mL} \times 100\%}{15.0\ \text{mg}} = 8.40\%$$

$$\text{DLE}\ (\%) = \frac{\text{weight of drug encapsulated in vesicles}}{\text{weight of drug in feed}} \times 100\%$$

$$= \frac{52.9\ \mu\text{g mL}^{-1} \times 23.7\ \text{mL} \times 100\%}{3.50\ \text{mg}} = 35.8\%$$

The release profiles of the free DOX (in the absence of vesicles) and the DOX-loaded polymer vesicles solution were measured in 0.01 M tris buffer at 37 °C, respectively. The release profile of the free DOX was obtained by measuring the fluorescence intensity of DOX during the dialysis process. DOX·HCl was dissolved in deionized water at 52.9 μg mL^{-1} (the same DOX concentration as in the DOX-loaded vesicle solution), then 9.0 mL of solution was divided equally into three tubes (cut off Mn = 8000−14000), and the solution was dialyzed against 80 mL of tris buffer solution. Fluorescence intensity was measured at the same intervals as in the drug loading test. As expected, the release percentage of the free DOX reached 34.1% in the first 0.5 h and up to 77.0% at 2 h. In contrast, the release profile of the DOX-loaded polymer vesicle showed retardation within 8 h (Figure 7).

DOI: 10.1021/acs.bioconjchem.5b00061
Bioconjugate Chem. 2015, 26, 725−734

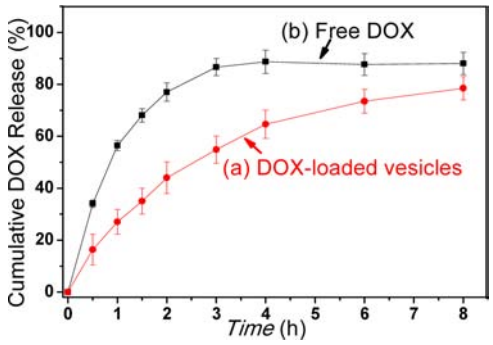

Figure 7. DOX release profiles of DOX-loaded vesicles and free DOX in 0.01 M tris buffer at pH 7.4 and 37 °C.

Cytotoxicity Study. The cytotoxicities of polymer vesicles were evaluated by a sensitive colorimetric CCK-8 assay against normal liver cells (L02) and cancer liver cells (7721) over 72 h. Living cells can be calculated by counting the amount of the formazan dye (a yellow-colored reduction product transformed from WST-8 (2-(2-methoxy-4-nitrophenyl)-3-(4-nitrophenyl)-5-(2,4-disulfophenyl)-2*H*-tetrazolium sodium salt) due to the dehydeogenase activities). The concentration of vesicles varies from 62 μg mL^{-1} to 500 μg mL^{-1}.

The polymer vesicles showed excellent antibacterial effect. Therefore, it is necessary to test the cytotoxicity of the peptide chains (the antibacterial part). It is noteworthy that the normal L02 cells remained with high metabolic activities at various copolymer vesicle concentrations (from 62 μg mL^{-1} to 500 μg mL^{-1}) after 72 h (Figure 8), which is similar to our previous work.[13] This is because of the high biocompatibility of the PCL chains and low cytotoxicity of peptide chains. Also, the vesicle morphology may decrease the cytotoxicity of antibacterial peptides and enhance the blood compatibility to eukaryotic cells.[13] Therefore, such antibacterial vesicles may have a wide range of applications in nanomedicine.

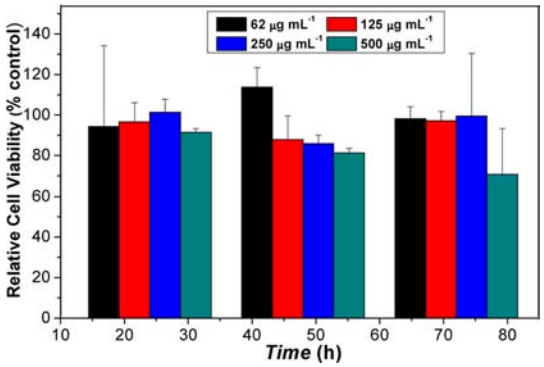

Figure 8. Cytotoxicity of polymer **8** vesicles against L02 cells (CCK-8 assays, n = 5).

Antitumor Activity Study. The antitumor activities of DOX-loaded polymer vesicles and free DOX were investigated by CCK-8 assay against 7721 liver cancer cells (Figure 9 and Figure S9, Supporting Information). The IC_{50} (inhibitory concentration to produce 50% cell death) value of the DOX·HCl in vesicles is 1.288 μg mL^{-1} (equiv 15.0 μg mL^{-1} DOX-loaded vesicles). This confirmed the excellent anticancer activity of the DOX-loaded polymer vesicles, indicating the successful delivery and release of DOX·HCl into the nucleus of 7721 liver cancer cells.

CONCLUSIONS

In conclusion, we have designed and synthesized a new peptide and PCL-based PCL$_{19}$-*b*-poly[Phe$_{12}$-*stat*-Lys$_9$-*stat*-(Lys-FA)$_6$] copolymer which can self-assemble into antibacterial vesicles as an "armed" drug carrier. The statistical copolymerization of Lys and Phe affords the antibacterial peptide vesicle coronas, which are highly effective against Gram-negative and Gram-positive bacteria. The biocompatible PCL forms the vesicle membrane, which showed a synergistic effect with antibacterial peptide to enhance its antibacterial activity and finally can be degraded and dissociated after drug release. More importantly, the FA-conjugated vesicles may guide the vesicles to the cancer cell for targeted drug transportation and release. Furthermore, the residual $-NH_2$ groups in the vesicle coronas can be further functionalized for further "upgrading". Overall, this low cytotoxic, biocompatible, potentially cancer-targeting antibacterial polymer vesicle is a promising vehicle in nanomedicine.

EXPERIMENTAL SECTION

Materials. *N*-ε-Benzyloxycarbonyl-L-lysine, L-phenylalanine, triphosgene, and hydrogen bromide (30% in acetic acid) were purchased from Shanghai Hanhong Chemical Co., Ltd. ε-Caprolactone (Aldrich) was dried azeotropically using anhydrous toluene prior to use. Hexane, stannous 2-ethylhexanoate (Sn(Oct)$_2$), trifluoroacetic acid (TFA), diethyl ether, tetrahydrofuran (THF), *N*,*N*-dimethylformamide (DMF), *n*-hexylamine, benzyl alcohol, dichloromethane, and methanol were purchased from Aladdin. DMF and THF were dried by reflux for 1 day in the presence of calcium hydride and sodium strips, respectively. Diisopropylethylamine (DIPEA) and *O*-(7-aza-

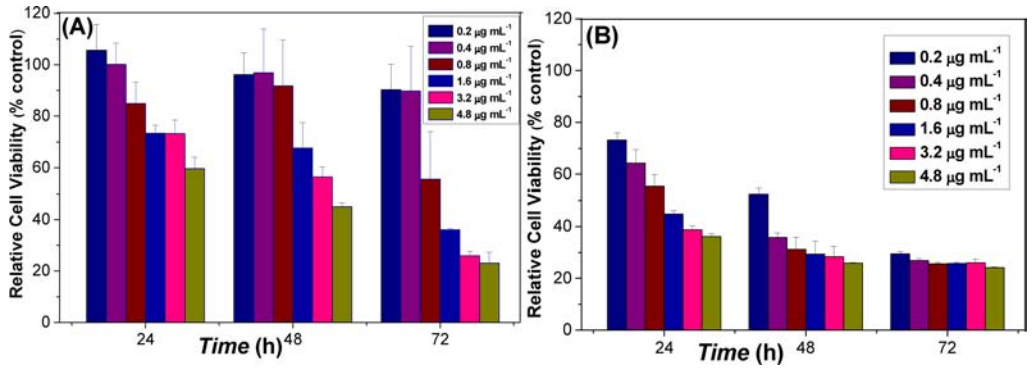

Figure 9. (A) Anticancer activity of DOX-loaded polymer ***8*** vesicles and (B) Free DOX against 7721 liver cancer cells (CCK-8 assays, n = 5).

DOI: 10.1021/acs.bioconjchem.5b00061
Bioconjugate Chem. 2015, 26, 725−734

benzotriazole-1-yl)-*N*,*N*,*N*,*N*′-tetramethyluroniumhexafluorophosphate (HATU) were purchased from Sigma-Aldrich. Doxorubicin hydrochloride (DOX·HCl; 98%; purchased from Xingcheng Chempharm Co., Ltd.), Gram-negative bacterium *E. coli* (ATCC35218), and Gram-positive bacterium *S. areus* (ATCC29213) were purchased from Nanjing Bianzhen Biological Technology Co., Ltd. Other chemicals were used without further purification unless otherwise specified.

Synthesis of Z-Lys-NCA Monomer (Monomer *1*). *N*-ε-Benzyloxycarbonyl-L-lysine (4.000 g, 14.27 mmol) and α-pinene (9.703 g, 71.30 mmol) were dissolved in 100 mL of anhydrous THF in a three-necked round-bottomed flask. Triphosgene (3.180 g, 10.71 mmol) was dissolved in 30.0 mL of anhydrous THF in a constant pressure funnel. The air in the whole device was exhausted by blowing argon. Then, triphosgene solution was added dropwise over a period of 1 h at 50 °C with the protection of argon. The mixture would turn gradually clear in 4 h. The mixture was precipitated by dropping into 500.0 mL of hexane with fast stirring. The crude product was dissolved in dry THF and recrystallized twice by dropping into vast hexane. The obtained solid could be used after 48 h of freeze-drying. Yield: ∼80%.

Synthesis of Phe-NCA Monomer (Monomer *2*). L-Phenylalanine (4.000 g, 24.21 mmol) and α-pinene (16.46 g, 121.1 mmol) were dissolved in 100.0 mL of anhydrous THF in a three-necked round-bottomed flask. Triphosgene (5.389 g, 18.16 mmol) was dissolved in 30.0 mL of anhydrous THF in a constant pressure funnel. Other procedures are similar to the synthesis of monomer *1*. Yield: ∼82%.

Synthesis of Poly[(Z-Lys)$_{15}$-*stat*-Phe$_{12}$] (Polymer *3*). Z-Lys-NCA (2.000 g, 6.540 mmol) and Phe-NCA (0.8300 g, 4.360 mmol) monomers were added into DMF (30.0 mL) in a dried flask. The mixture was stirred at room temperature in a vacuum for 6 h after the addition of the *n*-hexylamine initiator (44.0 mg, 0.044 mmol). The crude polymer *3* was obtained by precipitation in water. The excess DMF was removed by washing with water. Purified polymer *3* was obtained by freeze-drying for 48 h. Yield: ∼81%.

Synthesis of Poly[(Z-Lys)$_{15}$-*stat*-Phe$_{12}$]-NCO (Polymer *4*). Poly[(Z-Lys)$_{15}$-*stat*-Phe$_{12}$] (2.000 g) was dissolved in 10.0 mL of DMF in a flask in an anhydrous condition. After the addition of hexamethylene diisocyanate (HDI) (1.580 g), the mixture was stirred for 2 h at 0 °C. Poly[(Z-Lys)$_{15}$-*stat*-Phe$_{12}$]-NCO was precipitated in excess *n*-hexane, then the solid was dissolved in DMF again. The process was repeated three times in order to remove excess HDI. Poly[(Z-Lys)$_{15}$-*stat*-Phe$_{12}$]-NCO in DMF was ready for the next step.

Synthesis of PCL$_{19}$-OH (Polymer *5*). First, ε-caprolactone (5.000 g, 43.91 mmol) and toluene (50.0 mL) were added to a round-bottomed flask to remove the trace of water in an oil bath at 130 °C by azeotropic distillation. The solution was degassed with argon sparge for 30 min. Then, benzyl alcohol (0.2630 g, 2.434 mmol) and a drop of Sn(Oct)$_2$ catalyst were added. After stirring for 48 h at 110 °C, the reactor was cooled to room temperature to stop the reaction. PCL$_{19}$-OH was precipitated in excess methanol and repeated three times, and dried under vacuum for 2 days to afford polymer *5*. Yield: ∼81%.

Synthesis of PCL$_{19}$-*b*-Poly[Phe$_{12}$-*stat*-(Z-Lys)$_{15}$] (Polymer *6*). PCL$_{19}$-OH (0.9500 g) was dissolved in DMF (5.0 mL), and the mixture was added into the poly[(Z-Lys)$_{15}$-*stat*-Phe$_{12}$]-NCO DMF solution, then two drops of dibutyltin dilaurate were added in. After 12 h of reaction, the solution was dialyzed against deionized water for 24 h. The product was dried for the next step. Yield: ∼54%.

Synthesis of PCL$_{19}$-*b*-Poly(Phe$_{12}$-*stat*-Lys$_{15}$) (Polymer *7*). The mixture of PCL$_{19}$-*b*-Poly[Phe$_{12}$-*stat*-(Z-Lys)$_{15}$] and excess HBr (10.0 mL, 30% in acetic acid) was stirred for 4 h, then the solid was precipitated by dropping the mixture into diethyl ether and washed by diethyl ether and acetone five times. Finally, the turbid solution was dialyzed against deionized water for 48 h. The polymer was obtained by freeze-drying. Yield: ∼53%.

Synthesis of PCL$_{19}$-*b*-Poly[Phe$_{12}$-*stat*-Lys$_9$-*stat*-(Lys-FA)$_6$] (Polymer *8*). The PCL$_{19}$-*b*-poly(Phe$_{12}$-*stat*-Lys$_{15}$) (500.0 mg, 87.72 mmol) and folic acid (FA; 232.3 mg, 52.68 mmol) and *O*-(7-azabenzotriazole-1-yl)-*N*,*N*,*N*,*N*′-tetramethyluroniumhexafluorophosphate (HATU; 66.71 mg, 17.54 mmol) were mixed in dry DMF and stirred for 1 h. Then, diisopropylethylamine (DIPEA; 22.7 mg, 17.54 mmol) was added to the solution. The solution was stirred for another 24 h. Then, the solvent was removed under vacuum. The product was purified by precipitating into diethyl ether three times and dialyzing against deionized water for 24 h. The copolymers were finally obtained by freeze-drying for 48 h. Yield: ∼70%.

Synthesis of Poly(Phe$_{12}$-*stat*-Lys$_{15}$) (Polymer *9*). Poly-[(Z-Lys)$_{15}$-*stat*-Phe$_{12}$] (polymer *3*) and excess HBr (10.0 mL, 30% in acetic acid) were stirred for 4 h, then the solid was precipitated by dropping the mixture into the diethyl ether and washing by diethyl ether and acetone five times. Finally, the turbid solution was dialyzed against deionized water for 48 h. The polymer was obtained by freeze-drying.

Self-Assembly of PCL$_{19}$-*b*-poly[Phe$_{12}$-*stat*-Lys$_9$-*stat*-(Lys-FA)$_6$] (Polymer *8*) into Vesicles. Polymer *8* (9.0 mg) was dissolved in 3.0 mL of DMSO. A drop of TFA was added to break the hydrogen bond. Then, 6.0 mL of deionized water was dropped into the solution by a gastight syringe with violent stirring for 10 min. After another 12 h of stirring, the solution was dialyzed against deionized water for 24 h to remove the DMSO and TFA.

Enzymatic Biodegradation of Polymer *8* Vesicles. Polymer *8* vesicles consisting of PCL can be degraded in the presence of the lipase. The count rates of the polymer vesicle solution can reflect the degradation degree. The aqueous lipase solution (0.034 mL, 0.017 mL, and 0.009 mL; 5.0 mg mL^{-1}) was added into 1.66 mL of vesicles solution (0.05 mg mL^{-1}). Then, the mixture was put into an incubator at 37 °C to detect the variance of the count rate with certain intervals by DLS.

Preparation of DOX-Loaded Polymer *8* Vesicles. Polymer *8* (15.0 mg) and DOX·HCl (3.50 mg) was dissolved in 5.0 mL of DMSO, and a drop of TFA was added. Then, 10.0 mL of deionized water was added to the solution with continuous stirring. Then, the solution above was dialyzed against 1000 mL of tris buffer (0.01 M; pH 7.4) in a dialysis tube (cutoff M_n = 8000−14000) at 25 °C to remove the unloaded free drug, DMSO solvent, and TFA. The dialysis medium was renewed each 0.5 h in 3 h.

***In Vitro* Drug Release.** The *in vitro* drug release experiment was conducted according to the following protocol. After 3 h of dialysis, the vesicle solution was withdrawn and divided into 3 dialysis tubes (cutoff M_n = 8000−14000). Each tube contained 3.0 mL of DOX-loaded vesicles solution and was dialyzed against 80.0 mL of tris buffer (0.01 M; pH 7.4) in a beaker (100 mL) at 37 °C and at a stirring rate of 2000 r/min. At desired time intervals, 1.0 mL of release media was taken out from the beaker to test the fluorescence intensity (excitation at 461 nm

DOI: 10.1021/acs.bioconjchem.5b00061
Bioconjugate Chem. 2015, 26, 725−734

and emission at 591 nm). After the measurement, the release media were put back into the beaker. The cumulative release curve of DOX was obtained based on the calibration curve reported previously.[45] Three parallel experiments were carried out to minimize experimental error.

Antibacterial Test. Two different methods were used to measure the MICs of polymers ***8*** and ***9***. As a reference, polymer ***9*** is studied with a simpler method. For polymer ***9***, bacteria cells were grown overnight at 37 °C in broth medium to a mid-log phase and diluted to 10^4−10^5 colony forming unit mL^{-1}. The peptide solution was diluted in the bacterial solution range from 1000 to 8 μg mL^{-1}. Optical density absorbance was measured at 600 nm.

For polymer ***8***, polymer vesicles solution (30 mg mL^{-1}) was diluted to different concentrations using saline. Then, 1.0 mL of solution and 20 μL of microorganism solution were mixed in a conical flask at 37 °C. The optical densities of the microorganism solution were measured as a function of time. The control is only broth-containing bacterial cells. More details have been published in our recent articles.[13]

Critical Vesiculation Concentration (CVC). The CVC is defined as the lowest concentration of polymers to form vesicles in water. Pyrene was used as the probe to detect the vesicle formation. An initial solution of pyrene was made by dissolving pyrene (3.0 mg, 15 μmol) in acetone (25 mL). Nine centrifuge tubes were filled with 10 μL of pyrene solution. After evaporation of acetone, the polymer ***8*** vesicle solution was diluted with deionized water into different concentrations. Then, 4.0 mL of solution at each concentration was added into the centrifuge tubes and stirred overnight. Fluorescence intensities were recorded by exciting samples at 334 nm, using a 5 nm slit width for excitation and a 5 nm slit width for emission. The sample was scanned with an emission wavelength from 350 to 500 nm. The intensities of the I_1 (371.7 nm) were chosen as the vibronic bands. The intensity values were plotted against the log of the concentration of each polymer vesicle sample. The CVC was obtained by calculating the intersection of two regression lines programmed from the linear portions of the graphs.[45]

In Vitro* Stability of Vesicles in PBS and FBS.** The polymer ***8 vesicle solutions were incubated in PBS (0.01 M at pH 7.4) and FBS buffer solutions at different concentrations at 37 °C for 5 days. The hydrodynamic diameters of vesicles were measured by DLS to evaluate their stability.

Cytotoxicity Test. Normal liver cells (L02) and live cancer cells (7721) were chosen to test the cytotoxicity of the polymer vesicles and DOX-loaded vesicles through Cell Counting Kit-8 (CCK-8).[13] First, 100.0 μL of Dulbecco's modified Eagle's medium (DMEM) supplemented with 10% fetal bovine serum (FBS) was used to cultivate the L02 and 7721 cells in the well with the same density (4000 cells/well) for 24 h at 37 °C in a humidified 5% CO_2-containing atmosphere. Second, 20.0 μL of polymer vesicle and DOX-loaded vesicles solution with certain concentrations were added and incubated for 24, 48, and 72 h. The control group is untreated cells. Lastly, CCK-8 dye was added to each well, and the plates were incubated for another 1 h at 37 °C. Then, a microplate reader was used to measure the absorbance by dual wavelength spectrophotometry at 450 and 630 nm, and each treatment was repeated five times. The relative cell viability (%) was determined by comparing the absorbance at 450 nm with control wells containing only cell culture medium.

Characterization. *Proton Nuclear Magnetic Resonance (^1H NMR).* The spectra were recorded using a Bruker AV 400 MHz spectrometer, with DMSO-d_6, D_2O, or $CDCl_3$ as solvent and TMS as standard at room temperature. In some cases, CF_3COOD was added to break hydrogen bonding in polypeptides.

DLS. The DLS studies of aqueous polymer vesicles were performed using Nano-ZS 90 Nanosizer (Malvern Instruments Ltd., Worcestershire, UK) at a fixed scattering angle of 90°. Each reported measurement was conducted three times. Disposable cuvettes were used to analyze the aqueous aggregates solution. The data were processed by cumulative analysis of the experimental correlation function. The particle diameters were calculated from the computed diffusion coefficients using the Stokes−Einstein equation.

TEM. TEM images were taken with a JEOL JEM-2100F instrument at 200 kV equipped with a Gatan 894 Ultrascan 1 k CCD camera. The TEM samples were made by dropping 3 μL of diluted vesicle onto a carbon-coated copper grid and drying at ambient environment. Phosphotungstic acid (PTA; 1%, pH 7) solution was dropped onto a hydrophobic film (parafilm), and then the sample-loaded grids were laid upside down on the top of the PTA solution for 1 min, and the excess PTA solution was slightly blotted up through a filter paper. After that, the grids were dried under ambient environment overnight.

AFM. AFM was employed to verify the hollow structure (height contrast) of the polymer vesicle. The fresh silicon wafer was washed in the acetone under ultrasound for 10 min. The sample solution was diluted to 0.03 mg mL^{-1} and dropped (10 μL) onto the silicon wafer (1 × 1 cm^2) and dried at room temperature. The observation was conducted on a Seiko (SPA-300 HV) instrument operating in tapping mode at 200−400 kHz drive frequency.

UV−Vis Spectroscopy. UV−vis studies were conducted using an UV−vis spectrophotometer (UV-759S, Q/YXL270, Shanghai Precision & Scientific Instrument Co., Ltd.) with a scan speed of 300 nm min^{-1}. The absorbance and transmittance spectra of the vesicles were recorded in the range of 600 nm.

Fluorescence Spectroscopy. Fluorescence intensities of the cumulative DOX release of DOX-loaded vesicles were measured with a fluorescence spectrometer (excitation at 461 nm and emission at 591 nm) via a Lumina Fluorescence Spectrometer (Thermo Fisher).

GPC. Gel permeation chromatography (GPC) analysis was carried out with a Waters Breeze 1525 GPC analysis system with two PL mix-D columns and a light scattering detector, using THF as eluent at a flow rate of 1.0 mL at 25 °C.

■ ASSOCIATED CONTENT

Ⓢ Supporting Information

Additional ^1H NMR spectra and calculations, GPC trace, AFM images, DLS data and anticancer activity data against 7721 liver cancer cells. This material is available free of charge via the Internet at http://pubs.acs.org.

■ AUTHOR INFORMATION

Corresponding Author

*Phone: +86-21-6958 0239. Fax: +86-21-6958 4723. E-mail: jzdu@tongji.edu.cn.

Author Contributions

†M.W., C.Z., and J.C. contributed equally to this work.

DOI: 10.1021/acs.bioconjchem.5b00061
Bioconjugate Chem. 2015, 26, 725−734

Notes

The authors declare no competing financial interest.

■ ACKNOWLEDGMENTS

This work was supported by Shanghai 1000 Plan, Eastern Scholar Professorship, NSFC (21174107, 21274110, and 21374080) and Ph.D. Program Foundation of Ministry of Education (20110072110048).

■ REFERENCES

(1) Coates, A., Hu, Y., Bax, R., and Page, C. (2002) The future challenges facing the development of new antimicrobial drugs. *Nat. Rev. Drug. Discovery 1*, 895−910.

(2) Hancock, R. E. (2001) Cationic peptides: effectors in innate immunity and novel antimicrobials. *Lancet Infect. Dis. 1*, 156−164.

(3) Yao, D., Guo, Y., Chen, S., Tang, J., and Chen, Y. (2013) Shaped core/shell polymer nanoobjects with high antibacterial activities via block copolymer microphase separation. *Polymer 54*, 3485−3491.

(4) Qi, X. B., Zhou, C. C., Li, P., Xu, W. X., Cao, Y., Ling, H., Chen, W. N., Li, C. M., Xu, R., Lamrani, M., et al. (2010) Novel short antibacterial and antifungal peptides with low cytotoxicity: efficacy and action mechanisms. *Biochem. Biophys. Res. Commun. 398*, 594−600.

(5) Hancock, R. E. W., and Sahl, H.-G. (2006) Antimicrobial and host-defense peptides as new anti-infective therapeutic strategies. *Nat. Biotechnol. 24*, 1551−1557.

(6) Engler, A. C., Shukla, A., Puranam, S., Buss, H. G., Jreige, N., and Hammond, P. T. (2011) Effects of side group functionality and molecular weight on the activity of synthetic antimicrobial polypeptides. *Biomacromolecules 12*, 1666−1674.

(7) Hancock, R. E. W., and Scott, M. G. (2000) The role of antimicrobial peptides in animal defenses. *Proc. Natl. Acad. Sci. U.S.A. 97*, 8856−8861.

(8) Wang, M. Z., and Du, J. Z. (2014) Progress in syntheses and applications of polypeptides and polypeptide-based copolymers by NCA polymerization. *Acta Polym. Sin. 0*, 1183−1194.

(9) Rao, J., Luo, Z., Ge, Z., Liu, H., and Liu, S. (2007) "Schizophrenic" micellization associated with coil-to-helix transitions based on polypeptide hybrid double hydrophilic rod−coil diblock copolymer. *Biomacromolecules 8*, 3871−3878.

(10) Rao, J., Zhang, Y., Zhang, J., and Liu, S. (2008) Facile preparation of well-defined AB2 Y-shaped miktoarm star polypeptide copolymer via the combination of ring-opening polymerization and click chemistry. *Biomacromolecules 9*, 2586−2593.

(11) Zhou, C. C., Qi, X. B., Li, P., Chen, W. N., Mouad, L., Chang, M. W., Leong, S. S. J., and Chan-Park, M. B. (2009) High potency and broad-spectrum antimicrobial peptides synthesized via ring-opening polymerization of α-aminoacid-*N*-carboxyanhydrides. *Biomacromolecules 11*, 60−67.

(12) Wyrsta, M. D., Cogen, A. L., and Deming, T. J. (2001) A parallel synthetic approach for the analysis of membrane interactive copolypeptides. *J. Am. Chem. Soc. 123*, 12919−12920.

(13) Zhou, C. C., Wang, M. Z., Zou, K. D., Chen, J., Zhu, Y. Q., and Du, J. Z. (2013) Antibacterial polypeptide-grafted chitosan-based nanocapsules as an "armed" carrier of anticancer and antiepileptic drugs. *ACS Macro Lett. 2*, 1021−1025.

(14) Pegram, M. D., Konecny, G. E., O'Callaghan, C., Beryt, M., Pietras, R., and Slamon, D. J. (2004) Rational combinations of trastuzumab with chemotherapeutic drugs used in the treatment of breast cancer. *J. Natl. Cancer Inst. 96*, 739−749.

(15) Dorresteijn, R., Billecke, N., Schwendy, M., Pütz, S., Bonn, M., Parekh, S. H., Klapper, M., and Müllen, K. (2014) Polylactide-block-polypeptide-block-polylactide copolymer nanoparticles with tunable cleavage and controlled drug release. *Adv. Funct. Mater. 24*, 4026−4033.

(16) Olson, E. S., Aguilera, T. A., Jiang, T., Ellies, L. G., Nguyen, Q. T., Wong, E. H., Gross, L. A., and Tsien, R. Y. (2009) In vivo characterization of activatable cell penetrating peptides for targeting protease activity in cancer. *Integr. Biol. 1*, 382−393.

(17) Du, J. Z., and O'Reilly, R. K. (2009) Advances and challenges in smart and functional polymer vesicles. *Soft Matter 5*, 3544−3561.

(18) Feng, A. C., and Yuan, J. Y. (2014) Smart nanocontainers: progress on novel stimuli-responsive polymer vesicles. *Macromol. Rapid Commun. 35*, 767−779.

(19) Janib, S. M., Moses, A. S., and MacKay, J. A. (2010) Imaging and drug delivery using theranostic nanoparticles. *Adv. Drug Delivery Rev. 62*, 1052−1063.

(20) Sun, C., Lee, J. S. H., and Zhang, M. Q. (2008) Magnetic nanoparticles in MR imaging and drug delivery. *Adv. Drug Delivery Rev. 60*, 1252−1265.

(21) Davis, M. E., Chen, Z., and Shin, D. M. (2008) Nanoparticle therapeutics: an emerging treatment modality for cancer. *Nat. Rev. Drug. Discovery 7*, 771−782.

(22) Hu, J., and Liu, S. (2010) Responsive polymers for detection and sensing applications: current status and future developments. *Macromolecules 43*, 8315−8330.

(23) Hu, X., Hu, J., Tian, J., Ge, Z., Zhang, G., Luo, K., and Liu, S. (2013) Polyprodrug amphiphiles: hierarchical assemblies for shape-regulated cellular internalization, trafficking, and drug delivery. *J. Am. Chem. Soc. 135*, 17617−17629.

(24) van Dongen, S. F. M., de Hoog, H.-P. M., Peters, R. J. R. W., Nallani, M., Nolte, R. J. M., and van Hest, J. C. M. (2009) Biohybrid polymer capsules. *Chem. Rev. 109*, 6212−6274.

(25) Discher, D. E., and Eisenberg, A. (2002) Polymer vesicles. *Science 297*, 967−973.

(26) Hickey, R. J., Haynes, A. S., Kikkawa, J. M., and Park, S.-J. (2011) Controlling the self-assembly structure of magnetic nanoparticles and amphiphilic block-copolymers: from micelles to vesicles. *J. Am. Chem. Soc. 133*, 1517−1525.

(27) Hu, J., Zhang, G., and Liu, S. (2012) Enzyme-responsive polymeric assemblies, nanoparticles and hydrogels. *Chem. Soc. Rev. 41*, 5933−5949.

(28) Rogachev, A. A., Yarmolenko, M. A., Rogachou, A. V., Tapalski, D. V., Liu, X., and Gorbachev, D. L. (2013) Morphology and structure of antibacterial nanocomposite organic-polymer and metal-polymer coatings deposited from active gas phase. *RSC Adv. 3*, 11226−11233.

(29) Song, J., Kong, H., and Jang, J. (2009) Enhanced antibacterial performance of cationic polymer modified silica nanoparticles. *Chem. Commun.*, 5418−5420.

(30) Chong, H., Nie, C., Zhu, C., Yang, Q., Liu, L., Lv, F., and Wang, S. (2011) Conjugated polymer nanoparticles for light-activated anticancer and antibacterial activity with imaging capability. *Langmuir 28*, 2091−2098.

(31) Parkin, D. M. (2006) The global health burden of infection-associated cancers in the year 2002. *Int. J. Cancer 118*, 3030−3044.

(32) Mane, S. R., Rao, N. V., Chaterjee, K., Dinda, H., Nag, S., Kishore, A., Das Sarma, J., and Shunmugam, R. (2012) Amphiphilic homopolymer vesicles as unique nano-carriers for cancer therapy. *Macromolecules 45*, 8037−8042.

(33) Stuart, M. A. C., Huck, W. T. S., Genzer, J., Muller, M., Ober, C., Stamm, M., Sukhorukov, G. B., Szleifer, I., Tsukruk, V. V., Urban, M., et al. (2010) Emerging applications of stimuli-responsive polymer materials. *Nat. Mater. 9*, 101−113.

(34) Schatz, C., Louguet, S., Le Meins, J.-F., and Lecommandoux, S. (2009) Polysaccharide-*block*-polypeptide copolymer vesicles: towards synthetic viral capsids. *Angew. Chem., Int. Ed. 121*, 2610−2613.

(35) Mantovani, A. (2009) Cancer: inflaming metastasis. *Nature 457*, 36−37.

(36) Mantovani, A., Allavena, P., Sica, A., and Balkwill, F. (2008) Cancer-related inflammation. *Nature 454*, 436−444.

(37) Schindler, M., and Osborn, M. J. (1979) Interaction of divalent cations and polymyxin B with lipopolysaccharide. *Biochemistry 18*, 4425−4430.

(38) Storm, D. R., Rosenthal, K. S., and Swanson, P. E. (1977) Polymyxin and related peptide antibiotics. *Annu. Rev. Biochem. 46*, 723−763.

(39) Hu, X., Chen, X., Liu, S., Shi, Q., and Jing, X. (2008) Novel aliphatic poly(ester-carbonate) with pendant allyl ester groups and its

DOI: 10.1021/acs.bioconjchem.5b00061
Bioconjugate Chem. 2015, 26, 725−734

folic acid functionalization. *J. Polym. Sci., Part A: Polym. Chem. 46*, 1852−1861.
(40) Liang, B., He, M.-L., Chan, C.-y., Chen, Y.-c., Li, X.-P., Li, Y., Zheng, D., Lin, M. C., Kung, H.-F., Shuai, X.-T., et al. (2009) The use of folate-PEG-grafted-hybranched-PEI nonviral vector for the inhibition of glioma growth in the rat. *Biomaterials 30*, 4014−4020.
(41) Licciardi, M., Tang, Y., Billingham, N. C., Armes, S. P., and Lewis, A. L. (2005) Synthesis of novel folic acid-functionalized biocompatible block copolymers by atom transfer radical polymerization for gene delivery and encapsulation of hydrophobic drugs. *Biomacromolecules 6*, 1085−1096.
(42) Varkouhi, A. K., Scholte, M., Storm, G., and Haisma, H. J. (2011) Endosomal escape pathways for delivery of biologicals. *J. Controlled Release 151*, 220−228.
(43) Herzog, K., Müller, R. J., and Deckwer, W. D. (2006) Mechanism and kinetics of the enzymatic hydrolysis of polyester nanoparticles by lipases. *Polym. Degrad. Stab. 91*, 2486−2498.
(44) Zhang, Q., Remsen, E. E., and Wooley, K. L. (2000) Shell cross-linked nanoparticles containing hydrolytically degradable, crystalline core domains. *J. Am. Chem. Soc. 122*, 3642−3651.
(45) Chen, W. Q., and Du, J. Z. (2013) Ultrasound and pH dually responsive polymer vesicles for anticancer drug delivery. *Sci. Rep. 3*, DOI: 10.1038/srep02162.

DOI: 10.1021/acs.bioconjchem.5b00061
Bioconjugate Chem. 2015, 26, 725−734